Development of New Steel Damper for Seismic Retrofit of Existing Structures

Youngju Kim & Taesang Ahn
Seismic Isolation & Vibration Control Research Center, DRB Co. Ltd., Seoul, Korea (Email: kim.young.ju@drbworld.com)

Hyunggeun Kim
Seoul Metropolitan SH Corporation, Seoul, Korea

Dongwoon Jang
Construction Technology Development Dept., Ssangyong E&C Co. Ltd., Seoul, Korea

SUMMARY
The use of seismic energy dissipative devices for passive control is increasing exponentially in the recent years for both new and existing buildings. This paper proposes a new type of seismic damper based on yielding of a cantilever type steel damper for seismic retrofit of existing structures. The hysteretic behavior and energy dissipation capacity is investigated via component tests under cyclic loads. The experimental results indicate that the damping device has stable restoring force characteristics and a high energy dissipation capacity. Based on these results, a simple hysteretic model for predicting the load-displacement curve of the seismic damper is proposed.

Keywords: Steel damper, Seismic retrofit, Hysteretic behaviour, Energy dissipation capacity

1. INTRODUCTION

During a major earthquake, a large amount of energy is input into the building. The manner in which this energy is consumed in a structure determines the level of damage. If this energy can be controlled and dissipated in a manner independent of the structural components, the seismic performance and response of the structure will be substantially improved. This can be achieved by using passive control system of the structures. Structural control systems can be divided into three classes: passive, active, and semi-active. Passive control systems are structures equipped with energy dissipation devices that do not require an external power source for vibration response, while active or semi-active control systems are external power source for operation of actuators which supply control forces to the structure.

Within the passive control systems, this paper is focused on the development of simple, effective, and inexpensive energy dissipation devices feasible for massive application. Among passive energy dissipation systems, a steel damper is one of the most popular and has some advantages: no complicated technology is needed to manufacture it, it can easily be integrated on structures. Using a steel damper, the seismic demand on the structure is also reduced due to increase in the effective damping of the structures. Additional advantage of using energy dissipation devices is that after an earthquake, dampers can easily be replaced for retrofitting structures for future earthquakes. Numerous steel dampers have been proposed [1-4].

This paper investigates the use of the cantilever type steel plates as the energy dissipation device for seismic application as shown in Fig.1. The hysteretic behaviour and energy dissipation capacity is evaluated via component tests under cyclic loads. Finally, seismic performance test on large-scale structure was conducted to further verify the feasibility and effectiveness of the new seismic damper.

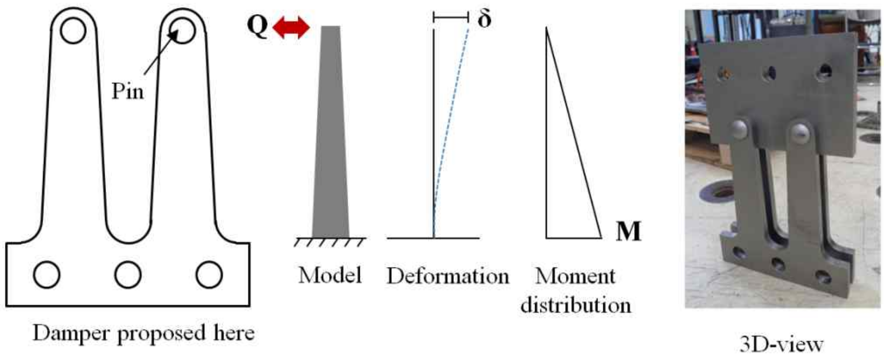

Figure 1. Seismic damper proposed

2. SEISMIC DAMPER DESIGN

Steel dampers proposed here can be used as part of chevron or X-type bracing systems and wall type systems (Fig.2). Steel devices dissipate energy through the relative horizontal displacement between the structural members. If cantilever type steel plates are used as shown in Fig.1, they will act as fixed-free beams such as cantilever beams and deform in one curvature. That is, the cantilever type steel plates are rigidly connected to a bottom plate by high strength bolts but are simply connected to a pinned top plate. Steel dampers are rounded at their fixed ends, thereby reducing stress concentration in reentrant-corners. To maximize the energy dissipation of the device, it is desirable that the plastic moment at any section be reached simultaneously. To achieve this condition, the geometry of the device must be optimized.

Assume a damper made of a single steel plate with a constant thickness *t* and a variable width *B(x)* as illustrated in Fig.3. When the plastic moment is reached at the ends of the device, the bending moment at any section of the device *M(x)* is given by:

$$M(x) = \frac{2M_p}{h}x = \left(\frac{x}{L}\right)\frac{tB^2}{4}F_y \text{, for } 0 \le x \le L \tag{1}$$

Where M_p is the plastic moment at the fixed end of the device, L is the length of the plate, B is the depth at the fixed end of the plate, x is the distance taken from the free end of the plate, and F_y is the yield strength of the steel. The plastic moment at any section of the plate $M_p(x)$ is given by:

$$M_p(x) = \frac{tB(x)^2}{4}F_y \tag{2}$$

To ensure simultaneous plastic yielding at all sections, when the plastic moment is reached at the ends of the plate, the moment acting at every section must be equal to the plastic moment of that section. Based on Eq.(1) and Eq.(2), the variation of the depth of the steel damper to maximize energy dissipation is given by:

$$B(x) = B\sqrt{\frac{x}{L}} \tag{3}$$

This optimum geometry is illustrated in Fig.3(a). Particularly, from a practical point of view, the depth of the plate cannot be zero at free end of a plate since the minimum depth of plates for a pinned connection must be needed. Assuming the minimum depth of free end '*b*', the geometry can be idealized as a linear variation of the width along the length of the plate to achieve the energy dissipation capacity corresponding to the optimized geometry of it. As shown in Fig.3(a), three types

of geometries are selected for a steel damper of which the ratios of depth of fixed end (B) to depth of free (pinned) end (b) of steel plates, B/b, are 1.25, 1.50 and 1.75, respectively.
For the purpose of predicting the yield strength and deformation of the steel damper, the steel plates were idealized as shown in Fig.3(b), where the round-shaped ends have been replaced with straight lines. By using these optimization and simplification, the yield strength of the steel damper can be obtained analytically as follows:

$$Q_y = \frac{tBF_{ye}}{4L'} \tag{4}$$

Where L' is the equivalent length indicated in Fig.3(b) ($L'=L+r^2/L_T$). F_{ye} is the expected yield stress. The yield displacement of the steel damper in relation to the depth ratio can be analytically expressed by the follow elastic-based equation.

$$\text{B=1.25,} \qquad \delta_y = \frac{16tB^2L'^3 F_y}{EI_N}\left(\ln\frac{5}{4} - \frac{11}{50}\right) \tag{5}$$

$$\text{B=1.50,} \qquad \delta_y = \frac{2tB^2L'^3 F_y}{EI_N}\left(\ln\frac{3}{2} - \frac{7}{18}\right) \tag{6}$$

$$\text{B=1.75,} \qquad \delta_y = \frac{16tB^2L'^3 F_y}{27EI_N}\left(\ln\frac{7}{4} - \frac{51}{98}\right) \tag{7}$$

Where E is the Young's modulus and I_N is the inertia moment of free end section.

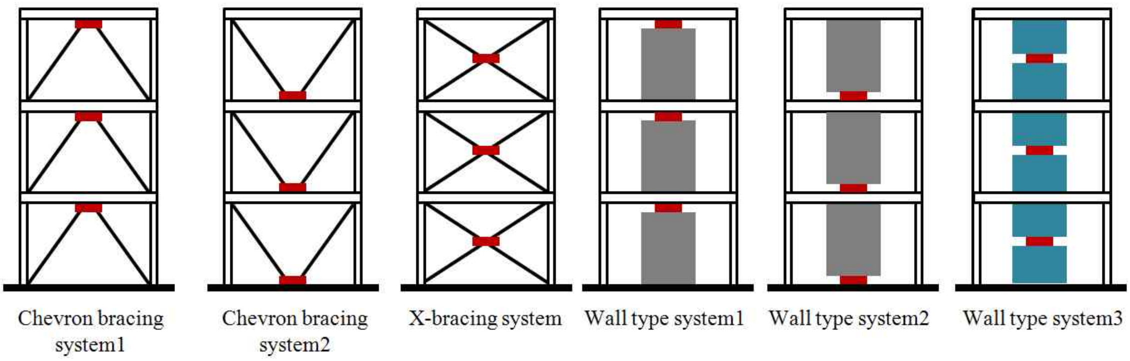

Figure 2. Use of dampers as part of bracing and wall type systems

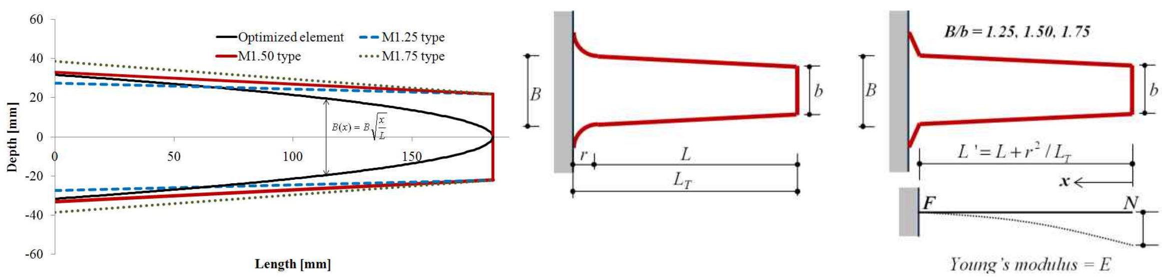

(a) Optimum geometry (b) Idealization of damper

Figure 3. Optimum geometry of steel damper

3. TEST PROGRAM

3.1 Specimens

To investigate the hysteretic behavior and energy dissipation capacity of the proposed damping device, component test were conducted. A total of 13 specimens as shown in Fig.4 were fabricated. It is composed of two cantilever type segments of steel plates. Three 26mm diameter holes were drilled and bolted for rigidity of fixed end, while two pinned connections were constructed at the top ends. Test parameters of specimens are thickness of steel plates, depth ratio and number of steel plates. All specimens were made of mild steel KS SS400 whose material yield stress obtained from standard coupon tests was on average 290 MPa.

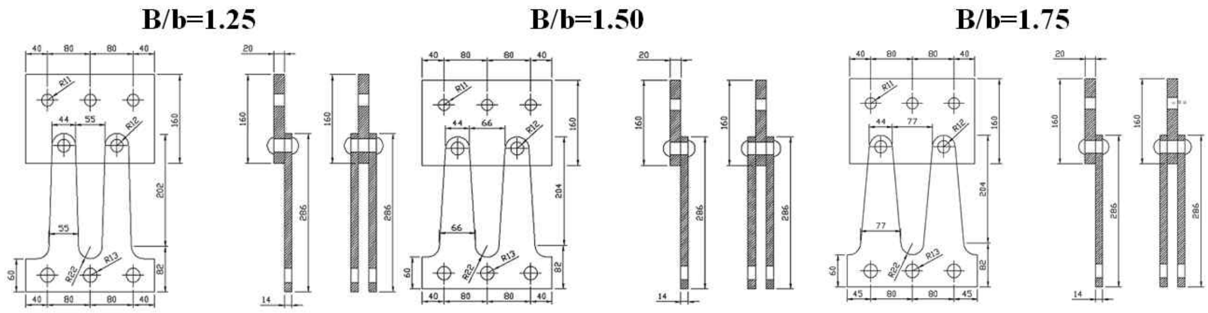

Figure 4. Test specimens

3.2 Test setup

The test setup shown in Fig.5 was designed to simulate the boundary conditions of various frame systems (Fig.2) under typical lateral loading. The test specimens were installed between both of L-frames, securely fastened by three high strength bolts on each side of steel damper. The setup, size, and other characteristics of the specimens were kept constant for the 13 tests, and the only variable considered was the loading history. Two patterns of cyclic displacements were applied to the specimens. In first test, specimens were subjected to cycles of incremental amplitude until they failed. Failure was assumed to occur when the strength started to decrease steadily under increasing forced displacements. After applying the elastic loading of $\pm 1\delta_y$, based on the displacement of the loading point, an incremental displacement control was applied, based on $\pm 2\delta_y$, $\pm 4\delta_y$, $\pm 8_y$, etc. Here, the term, δ_y, is the yield displacement corresponding to the plastic moment of the steel damper. In second test, the specimens were subjected to cycles of constant amplitude was 18mm, which was loaded with 20 fully reserved, irrespective of damper failure.

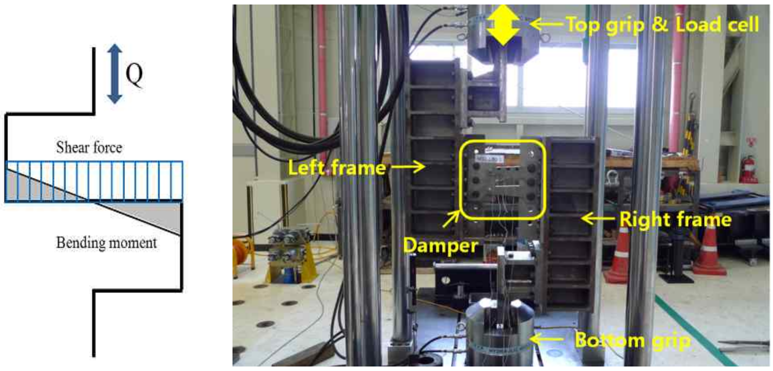

(a) Concept of test setup (b) Test setup

Figure 5. Test setup

4. TEST RESULTS

4.1 Hysteretic behaviour

Fig.6 shows the lateral load-displacement hysteretic curves obtained from the tests. All specimens deformed in a stable manner under the cyclic tests. The steel plates deformed in one curvature as expected. A positive sign refers to upward force and displacement.

It is clear that all specimens have yielded at small displacement and exhibited very stable hysteretic behaviour and the shape of the loops which close to a rectangular indicates high energy dissipation capacity. Strength degradation started to appear when cracks slowly formed at the ends of rounded corner of fixed ends due to stress concentration, which propagated longer and wider during the test until the specimen reached fracture. The tests were stopped after steel plates completely fractured and the load sustained was significantly reduced. Test results showed that in terms of ductility, specimens whose depth ratios (B/b) are 1.25 were inferior to specimens whose depth ratios are 1.50 or 1.75.

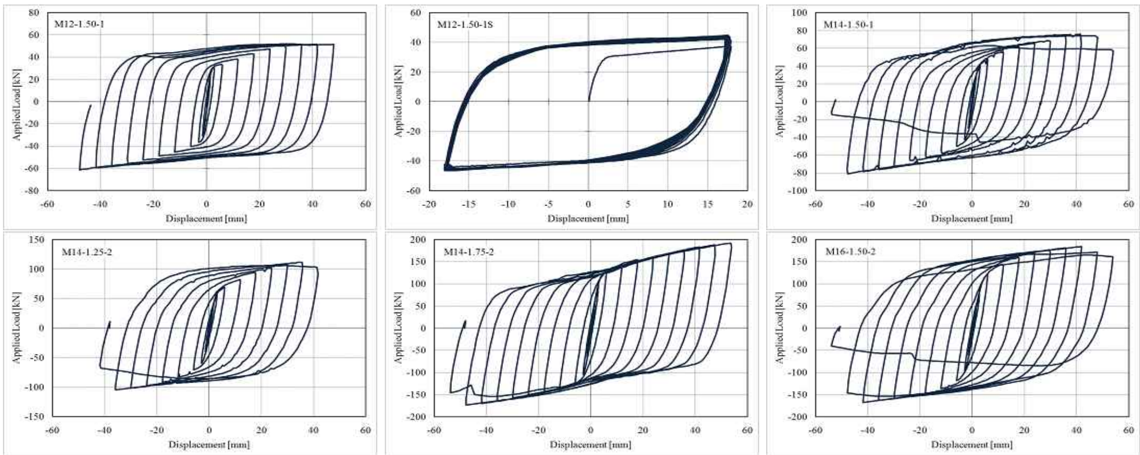

Figure 6. Load-displacement hysteresis for cyclic test specimens

Figure 7. Specimens at failure

4.2 Prediction of load-displacement curve

Load-displacement hysteresis loops of steel dampers under cyclic loading can be decomposed as skeleton curve and Bauschinger curve [5]. As shown in Fig.8, the skeleton curve is obtained by connecting parts of the load-displacement relationship sequentially when the damper first experienced its maximum load. To predict the load-displacement curve, the skeleton curves obtained from the tests in the positive and negative domains were taken in absolute value and normalized by Q_y and δ_y calculated as shown in Fig.9. Based on Eqs.(4)~(7), drawn in Fig.9 is the approximated bilinear skeleton curve whose normalized second stiffness is $K_2=1/65$ from test results. This result indicates that from the comparison of load-displacement curves, the theoretical model adequately describes the behaviour of the proposed steel damper.

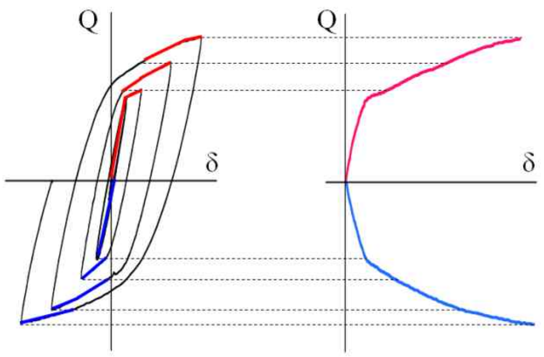

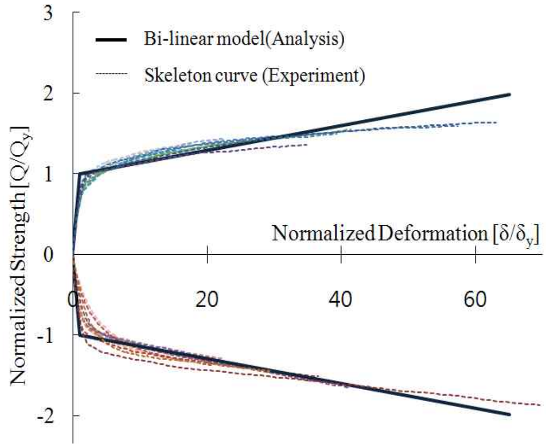

Figure 8. Skeleton curve

Figure 9. Approximate skeleton curve

4.3 Energy dissipation

To investigate the effect of test parameters on the energy dissipation capacity of dampers, the bar charts for dissipated energy were shown in Fig.10. Dissipated energy of specimens with depth ratio (B/b) of 1.5 or 1.7 is higher than that of specimens with depth ratio of 1.25. Specimens with depth ratio of 1.25, which have steel plates with the least depth variation, dissipated energy very poorly and failed at a relatively low cumulated displacement. It can be seen from Fig.10 that as the depth ratio and number of steel plates increase, the energy dissipation capacity increases, while there is no effect of the thickness of steel plates on energy dissipation capacity.

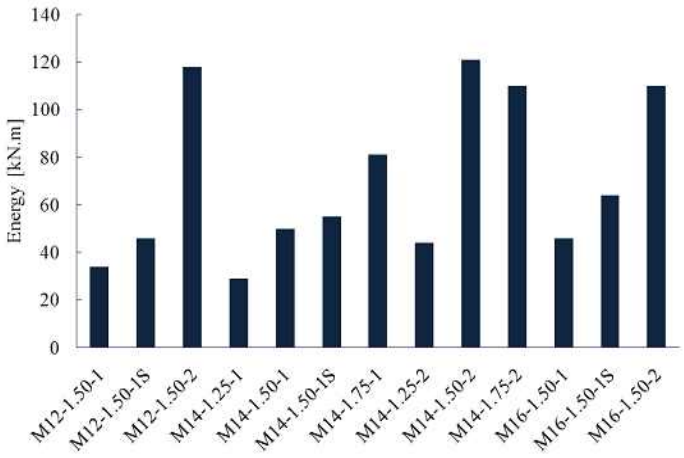

Figure 10**.** Dissipated energy

5. CONCLUSIONS

This paper describes the development of a new innovative energy dissipation device with cantilever type geometry. The proposed device dissipates input energy by flexural yielding of a series of cantilever type steel plates. All 13 cyclic tests were conducted. Cyclic test demonstrated stable hysteretic behaviour and dissipated significant amount of energy. The load-displacement of the device can be easily predicted by principle structural mechanism analysis, resulting that the design of the device can be easily extended to suit particular needs. Finally, devices with higher depth and number of steel plates behave more ductile, while devices with lower depth of steel plates suffer from earlier failure.

REFERENCES

Benavent-Climent, A., Morillas, L. and Vico, J.M. (2010). A study on using wide-flange sedtion web under out-of-plane flexural for passive energy dissipation. Earthquake *Engineering and Structural Dynamics.* **40:5**, 473-490

Black, C.J., Makris, N. and Aiken, I. (2004). Component testing, seismic evaluation and characterization of buckling-restrained braces. *Journal of Structural Engineering*. **130:6**, 880-894

Constantinou, M.C. and Symans, M.D. (1993). Seismic response of buildings with supplemental damping. *Journal of Structural Design of Tall Buildings*. **2**, 77-92

Chan R. W. K. and Albermani, F. (2008). Experimental study of steel slit damper for passive energy dissipation. *Engineering Structures*. **30:4**, 1058-1066

Kato, B., Akiyama, H. and Yamanouchi, H. (1973). Predictable properties of structural steels subjected to incremental cyclic loading. *IABSE Symposium on Resistance and Ultimate Deformability of Structures Acted on by Well Defined Loads*, Lisbon, Portugal, 111-124